An interpretation of size-scale plasticity in geometrically confined systems

H. D. Espinosa*†, S. Berbenni*‡, M. Panico*, and K. W. Schwarz§

*Department of Mechanical Engineering, Northwestern University, 2145 Sheridan Road, Evanston, IL 60208-3111; and §IBM Watson Research Center, Yorktown Heights, NY 10598

Communicated by Zdenek P. Bazant, Northwestern University, Evanston, IL, October 3, 2005 (received for review April 19, 2005)

The mesoscopic constitutive behavior of face-centered cubic metals as a function of the system characteristic dimension recently has been investigated experimentally. Strong size effects have been identified in both polycrystalline submicron thin films and single crystal micro pillars. The size effect is manifested as an increase in strength and hardening rate as the system dimensions are decreased. In this article, we provide a mechanistic interpretation for the observed mesoscopic behavior. By performing 3D discrete dislocation dynamics simulations of grains representative of the system microstructure and associated characteristic dimensions, we show that the experimentally observed size effects can be qualitatively described. In these simulations, a constant density of dislocation sources per unit of grain boundary area is modeled by sources randomly distributed at grain boundaries. The source length (strength) is modeled by a Gaussian distribution, in which average and standard deviation is independent of the system characteristic dimension. The simulations reveal that two key concepts are at the root of the observed plasticity size effect. First, the onset of plasticity is governed by a dislocation nucleation-controlled process (sources of various length, i.e., strengths, in our model). Second, the hardening rate is controlled by source exhaustion, i.e., sources are active only once as a result of the limited dislocation mobility arising from size and boundary effects. The model postulated here improves our understanding of why ''smaller is stronger'' and provides predictive capabilities that should enhance the reliable design of devices in applications such as microelectronics and micro/nano-electro-mechanical systems.

thin films | dislocation dynamics | strengthening

At the mesoscale, material behavior depends strongly on the system characteristic dimensions, e.g., material grain size, film thickness, etc. Size-scale plasticity has recently been the focus of research on both of these aspects. Concerning the material grain size effect, extensive research has been pursued on the mechanical behavior of nanocrystalline materials for which the grain size is on the order of 30 nm or smaller. For these systems, grain size effects and deviations from the classical Hall-Petch law have been identified (1). The size effect was attributed to a transition in deformation mechanism from a dislocation-dominated regime to grain boundary sliding (2). Another equally strong size effect, at constant grain size, has been correlated to sample dimensions. The so-called membrane deflection experiment (MDE) was used in the characterization of freestanding polycrystalline face-centered cubic (f.c.c.) thin films subjected to pure uniform tension (3, 4). In ref. 5, important size effects were reported, in the absence of macroscopic strain gradients, for Cu, Al, and Au films when the film thickness was varied from 0.2 to 1 μm. The films were deposited by e-beam evaporation and exhibited an average grain size of $\approx$200 nm independent of the film thickness. These studies showed that the material yield stress scales with the film thickness h and that its ductility decreases as this dimension decreases. A similar type of size effect has been reported for single crystalline micro pillar f.c.c. metals, with diameters ranging from 0.5 to 40 μm, tested in pure compression (6, 7). In such cases, traditional continuum plasticity models and their recent extensions (8, 9) to include strain gradient effects do not appear to be sufficient to explain the observed experimental phenomena. In both of these examples, size-scale plasticity is attributed to the dimensions of the sample that affect the nucleation and propagation of dislocations within the material. The objective of this article is to provide a scientific explanation for the observed plasticity size effect resulting from structure dimensional constraints. This issue is of particular interest in the context of thin films used in micro and nano-electro-mechanical systems and microelectronic devices. For instance, the microelectronics industry has identified challenges associated with interconnect structures as the finest wiring levels used for this purpose continue to shrink. Currently this wiring has a width of 90 nm, but projections of 45 nm by 2010 and 25 nm by 2015 have been made. Hence, prediction of mechanical properties at these scales is highly needed for the reliable design of next-generation electronic systems.

Our study is based on a number of experimental observations and discrete dislocation dynamics (DDD) simulations. It is known that size plays a direct role on the probability of finding a site for dislocation nucleation. In our model, dislocation nucleation is accounted for by a distribution of sources with various activation stresses. The dislocation density per unit grain boundary area is maintained constant with the source length (strength) and location statistically modeled by a Gaussian distribution with a constant average and standard deviation. By means of this model, we will show that, by changing the amount of surface where dislocations can nucleate, strong size affects result. Another implication of our probabilistic dislocation nucleation model on interfaces is that samples with the same composition and average grain size can exhibit different behaviors because of the discreteness of source sites and variability of activation stress. In this sense, for small volumes of materials, strength can be described only statistically, very much as is the case for brittle materials. Only when the so-called bulk response is achieved the yield strength of the material becomes deterministic or, in other words, the fluctuation in its value is very small and can be neglected. Indeed, a direct comparison of the tensile response of submicronic freestanding thin films with thick (or bulk) ones with self-similar experiments show that the yield and postyield behavior exhibit statistical variations only in the case of submicronic films (this work and ref. 5).

Experimental Results

We begin by reporting experimental evidence obtained with the MDE technique consisting of the direct tensile stressing of

Conflict of interest statement: No conflicts declared.

Abbreviations: MDE, membrane deflection experiment; f.c.c., face-centered cubic; DDD, discrete dislocation dynamics; TEM, transmission electron microscopy; SEM, scanning electron microscopy.

†To whom correspondence should be addressed. E-mail: espinosa@northwestern.edu.

‡Present address: Laboratory of Physics and Mechanics of Materials, Centre National de la Recherche Scientifique, Ecole Nationale Supérieure d'Arts et Métiers, Technopole, 57078 Metz Cedex, France.

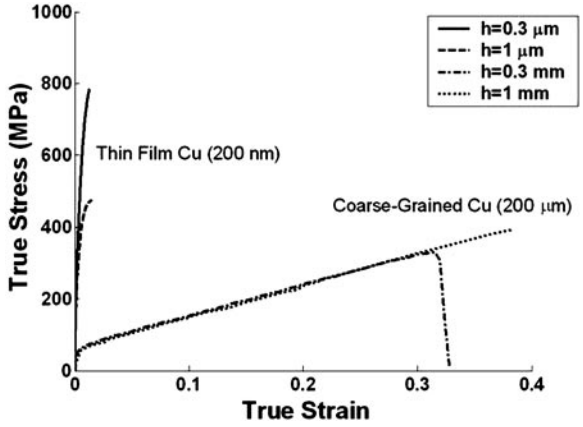

Fig. 1. Self-similar experiments in pure tension Cu films. Comparison between the mechanical response of submicronic ultrafine-grained thin films (MDE) and millimeter-thick coarse-grained films (Fullam tensile stage).

submicronic freestanding f.c.c. thin films. A detailed description of this experimental technique is given in refs. 3 and 4**.** Measured stress-strain curves for 0.3- and 1-μm-thick Cu films are shown in Fig. 1. The measured elastic modulus ranges from 125 to 129 GPa, which is consistent with the bulk crystal properties. Moreover, several size effects have been identified in the plastic deformation regime. First, the stress leading to the onset of plasticity is a strong function of the film thickness. Second, the strain hardening rate is observed to increase as the film thickness is decreased. The dominant geometrical constraint appears to be the film thickness because the grain size is kept approximately the same ($\approx$200 nm) and the influence of the sample width on the mechanical response is weaker and within statistical variations (5). Note that similar size effects have also been observed for Al and Au (5).

To further investigate the observed plasticity size-scale effects, e.g., in Cu films, we tested self-similar specimens until failure in tension occurred. The experiments were conducted by using a miniature tensile stage (Fullam, Latham, NY) equipped with a 2,000-lb load cell. The specimens were machined out of a copper foil and processed to have all of the characteristic dimensions (thickness, grain size) 1,000 times larger than the specimens used in the MDE. As a result, the number of grains through the thickness was about the same, but the surfaces of grain boundaries were increased 1 million times! The setup was placed under an optical microscope, and pictures were taken through the stretching process to keep track of deformations at the grain level. The specimen surface roughness was used to determine local strains by means of digital image correlation. Fig. 1 compares the stress-strain responses for coarse-grained films with thicknesses of 0.3 and 1 mm (using the Fullam tensile stage) with the ones for ultrafine-grained thin films with thicknesses of 0.3 and 1 μm (using the MDE). No size effect is observed in tension for the coarse-grained films, average grain size of 200 μm, whereas a "dramatic" size effect is observed in the submicronic ultrafine-grained thin films as previously stated. Movies 1 and 2, which are published as supporting information on the PNAS web site, show the evolution of the microstructure, including massive plastic deformations and local deformations in excess of 100%. The features are similar to plastic deformation within bulk polycrystalline metals where dislocations nucleate and propagate at relatively low levels of deviatoric stress, forming multiple slip lines across the grains.

The deformation mechanisms in the submicronic films are envisioned to be more complex in the sense that they are size dependent. Postmortem transmission electron microscopy

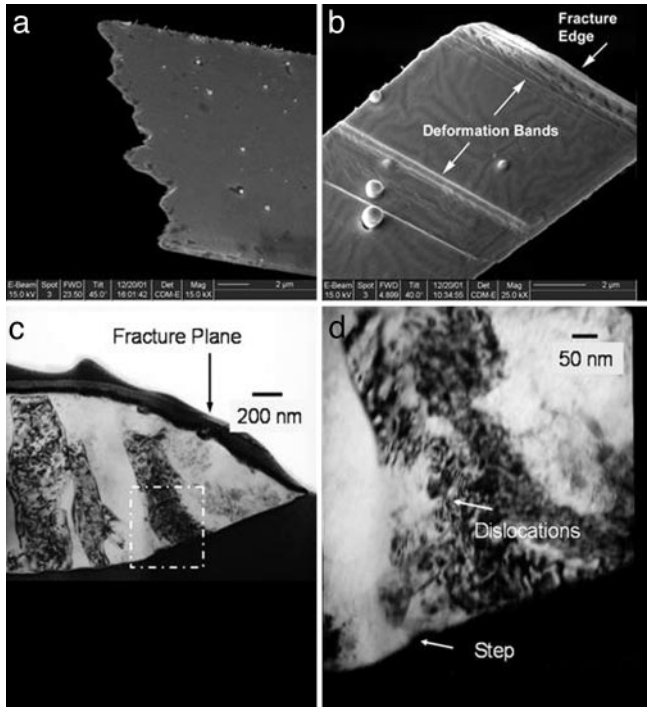

Fig. 2. TEM and SEM observations on MDE-tested Au films. (*a* and *b*) Study of the plastic activity of 0.3-μm-thick Au films (*a*) (SEM picture showing the fracture surface) and 1-μm-thick Au films (*b*) (SEM picture showing large deformation slip bands close to the fracture edge). (*c*) Cross-sectional TEM view of fracture region. (*d*) High-aspect-ratio grain exhibiting dislocation network.

(TEM) and scanning electron microscopy (SEM) observations on MDE-tested Au films were performed to gain insight into the origin of the size-scale experimental observations. SEM observation of the 0.3-μm-thick Au films reveals no major plastic activity as evident from the smoothness of the surface of the specimen near the fracture plane (Fig. 2*a*). TEM cross-sectional views of the same specimen display some residual dislocation networks within a few isolated grains with a decrease in dislocation activity from the fracture surface. TEM images before testing revealed an initial grain structure of the film basically free of dislocations. For 1-μm-thick Au films, significant plastic activity is evident in the SEM images of the specimen surface (Fig. 2*b*). The TEM cross-sectional views of the same specimen (Fig. 2 *c* and *d*) show a residual dislocation pattern only within grains with high aspect ratios. This finding suggests that dislocations moved mainly to the free surfaces, and they form networks only when the probability of forming dislocation junctions increases. We will come back to this feature later in the discussion of the DDD simulation results.

For the case of electron beam-evaporated 0.26-μm-thick Cu freestanding films, similar results were obtained in *in situ* TEM tensile tests (10). The stress level at the onset of plastic deformation and the rate of hardening were similar to those reported in ref. 5. In these *in situ* TEM studies, the films exhibited limited plasticity with dislocation nucleation at the grain boundaries. Dislocations were observed to sweep the grains and leave no trace within the crystal. Based on this mechanism and the measured plastic strain before failure, Keller *et al.* (10) concluded that only one dislocation every three or four grains was needed at the onset of yielding. In turn, this count resulted in a mobile dislocation density ranging from 2×10^9 to 8×10^9 m^{-2}. Their observations are consistent with our postmortem TEM observations and support the idea that plastically flowing grains

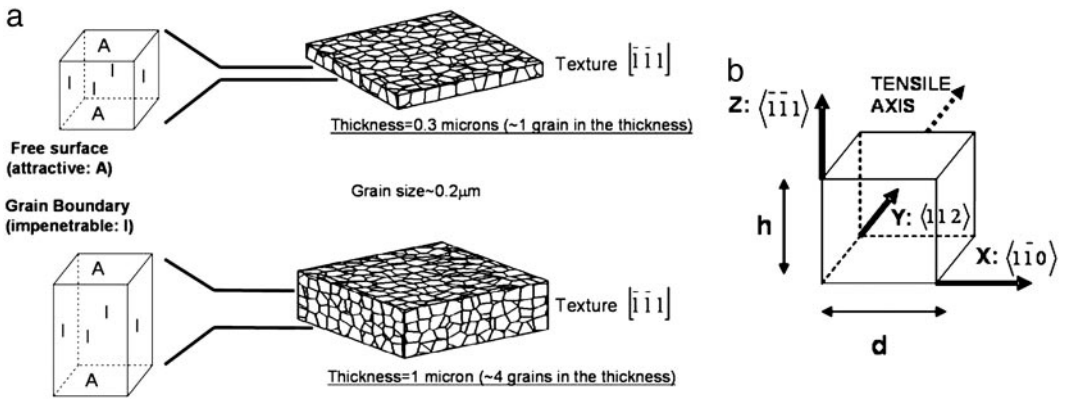

Fig. 3. Problem definition for DDD calculations. (*a*) Columnar grains simulating by rectangular boxes with various heights. (*b*) Present study: single crystal (grain) considered as a rectangular box [thickness: h; grain size: d with a crystallographic direction $\langle \bar{1}\bar{1}1 \rangle$ perpendicular to the film plane (consistent with the strong $\langle 111 \rangle$ texture of the film) and with an applied tensile loading parallel to the $\langle 112 \rangle$ direction (arbitrary)]. The sides are impenetrable to simulate grain boundaries, and the top and bottom faces are attractive to represent free surfaces.

do not develop strain hardening beyond stage I. It is worth mentioning that *in situ* TEM tensile tests reported in ref. 11 for sputtered pure Al and Au 0.1 μm-thick freestanding films resulted in a nonlinear elastic behavior that was attributed to grain boundary compliance. In such experiments, the grain size was smaller than in the studies reported in refs. 5 and 10, and it varied with film thickness. Haque and Saif (11) also reported that dislocation activity was observed in the largest grains within the material microstructure, but that no activity was observed when the grain size was 50 nm or smaller. These observations are in agreement with the current understanding of plasticity in nanocrystalline and ultrafine-grained metals.

The Computational Model

Classical crystal plasticity models are relevant for capturing the size-independent plastic deformation of thick films (multicrystals) in the millimeter range, but they are unable to show the dramatic size effects observed in thin films and micropillars. Extensions of these models using phenomenological continuum strain gradient theories are also found to be limited for applications in the submicron range (12). On the other hand, molecular dynamics simulations are not suitable for analyzing samples with average grain sizes of $\approx$200 nm, as in our case, because of the computational cost of this technique. For these reasons, it seems that the use of the DDD technique to simulate the mechanisms of activation (nucleation) and propagation of dislocations in geometrically confined volumes is ideal toward correlation between system characteristic dimensions and mesoscopic stress-strain response. Size-scale effects in single crystal films have been reported by using a 2D model (13) but considering only edge dislocations parallel to each other, which prevent more complex 3D phenomena to develop such as line tension effects. Three-dimensional effects were included in ref. 14 by modeling f.c.c. thin films on substrates with Frank-Read sources. Likewise, DDD has recently been used to determine the interaction between matrix components and collinear interaction useful in the formulation of constitutive crystal plasticity models for bulk polycrystals (15).

In this work, we focus on an interpretation of size-scale effects in confined volumes corresponding to polycrystalline freestanding thin films. We point out that the main purpose of this work is not to directly compare experiments and simulations but to postulate a simplified model based on the currently available mesoscale tools. In this regard, our analysis is essentially qualitative. We believe that this approach, while neglecting minor features of the problem, is nonetheless able to capture the essential characteristics of the discrete mechanisms involved.

The fully parallelized code PARANOID (16, 17) was used. This 3D code tracks the motion of dislocations by placing a sequence (mesh) of tracking points (or nodes) on the dislocations and considering external, interaction, and boundary forces on each dislocation segment. The numerical treatment of free surface forces on dislocation segments, with arbitrary Burgers vector orientations, is based on the Lothe formula. This formula provides the force per unit length acting on a dislocation as a result of the existence of a planar infinite free surface. For a discussion of its implementation in PARANOID and the accuracy of this boundary treatment, see ref. 16.

The PARANOID code is able to run in a highly resolved manner in which the point spacing can adapt down to atomic dimensions, making it very efficient for the study of the activation and motion of multiple dislocation sources. The mesoscopic response of a freestanding polycrystalline Cu thin film subjected to pure tension is studied here. The experimentally tested films exhibited one or more grains through the thickness, as schematically represented in Fig. 3*a*. In our analysis and because of current limitations of DDD implementations, including the one in PARANOID, we define a computational cell made of a single crystal, i.e., we do not include grain boundaries at the interior of the cell. The computational cell, displayed in Fig. 3*b*, consists of a rectangular box formed by a square area d^2 (with d being the grain size: 0.2 μm in the simulations) and a height h mimicking the thickness of the polycrystalline film. Note that this geometry is indeed present in some grains of the tested films, i.e., grains exhibiting high aspect ratios (Fig. 2*c*). The lateral faces of the box are modeled as impenetrable surfaces (grain boundaries), whereas the top/bottom faces are modeled as attractive to mimic the property of free surfaces. The crystallographic orientations are chosen to match the observed strong $\langle 111 \rangle$ texture for polycrystalline films in the direction normal to the film plane (5). An applied uniaxial tensile loading in the $\langle 112 \rangle$ direction (arbitrary) is prescribed. In principle and because the thin film has grains with various crystallographic orientations, other loading orientations should be simulated and averaged to describe the macroscopic stress-strain response of the thin film. Because in this work we model the phenomenon in 3D, such an endeavor is computationally too expensive, so we do not perform such an average. However, taking into account that we have randomly generated the grain boundary sources, i.e., random in terms of Burgers vectors and slip planes, and that we average three such

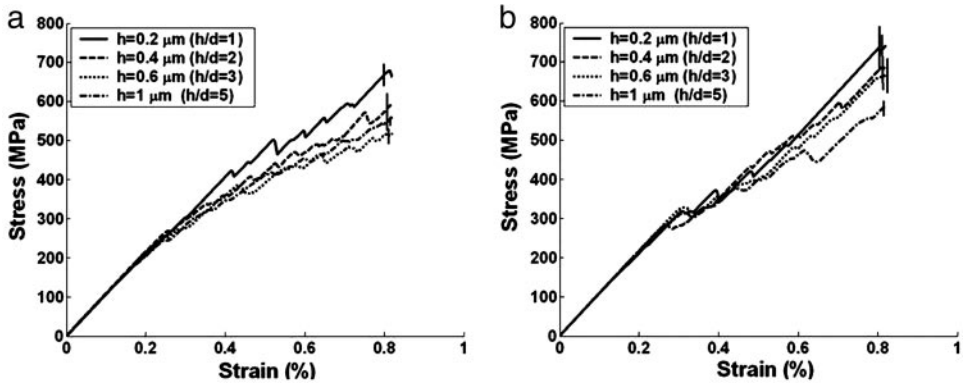

Fig. 4. Thickness effect obtained by DDD calculations for different thicknesses (h = 0.2, 0.4, 0.6, and 1 μm) considering a freestanding columnar grain. The error bars represent the statistical scatter of different runs at the end of the simulation for each sample. (*a*) Source density = 2.4×10^4 per cm. (*b*) Source density = 0.8×10^4 per cm.

manifestations in each case, the loading orientation effect is expected to be of minor significance.

In postulating an explanation for the observed plasticity size-scale effects, we will use dislocation sources randomly distributed only at grain boundaries. This assumption is in direct contrast with the study reported in ref. 14 where volume sources were used. The sources are not Frank-Read sources in the traditional sense because they do not possess the multiplicative character normally associated to these sources. As we will show later, active sources bow within the slip plane and are either absorbed by free surfaces or form dislocation junctions with dislocation segments stored at grain boundaries. We assume that for a grain size <200 nm grain boundary dislocation sources are the main origin of plastic activity. This assumption is rooted in a large body of experiments reported in the literature, for instance, in ref. 18, Cheng *et al.* highlight the existence of four ranges of grain sizes in f.c.c. metals for which distinct plastic deformation mechanisms exist. In the so-called "ultrafine" regime, which is the case of the tested freestanding submicron thin films, grain boundary dislocation sources appear to be predominant. In ref. 18, it is also suggested that the upper limit of this material behavior may be up to 1 μm. Only in microstructures possessing an average grain size above this value volume dislocation sources are expected to play a significant role in the plastic process. This assumption is well supported by a number of TEM experimental observations and atomistic simulations. For instance, in the *in situ* TEM tensile tests reported in ref. 10, the limited ductility of the films during straining is explained by a low number of available dislocation sources with the most likely sites for nucleation being grain boundaries. This feature is also consistent with other *in situ* TEM observations showing dislocations bowing away from grain boundaries and moving outward from the grains during straining (19, 20). Likewise, atomistic simulations of nanocrystalline copper with grain sizes ranging from 5 to 50 nm (21) revealed that most of the dislocations are emitted by grain boundaries. We recognize that for computational cells with small aspect ratios the probability of nucleating dislocations at the free surfaces increases. It is known that atomic roughness on the surface of the film, which results from the microfabrication process, can act as stress concentrators and nucleation sites. However, quantification of the effect of atomic roughness strength (step height) on dislocation nucleation threshold stress is very limited. Moreover, *in situ* TEM observations of dislocation activity in electron transparent films (an ultrasmall aspect ratio case) point at grain boundaries as the dominant source for dislocation nucleation. For these reasons, and although in principle our model can easily handle free surface dislocation sources, in the present study of thin films we restrict the nucleation sites to grain boundaries.

The effect of the thickness and the aspect ratio of a columnar grain on the mesoscopic stress-strain response is investigated by randomly distributed dislocation sources at the grain boundaries. A constant density per unit area of $\approx 2.4 \times 10^4$ cm^{-1} is used. The idea of a constant dislocation density per unit area is supported by atomistic simulations (22), which show that the number of dislocation sources per unit grain boundary area saturates to a constant value when the grain size increases beyond 20 nm. In our investigation, the source length follows a Gaussian distribution with a mean value of 0.08 μm and a standard deviation of 0.02 μm. Four different film thicknesses are examined (h = 0.2, 0.4, 0.6, and 1 μm) while the grain size is kept constant to d = 0.2 μm, which results in four different columnar grains with aspect ratios of 1, 2, 3, and 5, respectively. For each thickness, we performed three runs with different initial random source configurations. The stress-strain curves for the three calculations have been averaged to minimize fluctuations associated to the statistical nature of the sample. The averaging has the physical meaning of representing three manifestations of the ensemble of grains in the thin film. Ideally, if the computational cost would not be an issue, one should perform an average with a large number of manifestations more representative of the tested films including other loading directions. Likewise, a distribution in grain sizes would be needed.

Results and Discussion

In Fig. 4, we plot stress-strain curves for four film thicknesses, at constant grain size of 200 nm, and two initial dislocation densities. These stress-strain curves present stress drops, which are correlated to the grain boundary emission of dislocations on particular slip systems. Results (shown in Fig. 4*a*), corresponding to an initial dislocation density of 2.4×10^4 cm^{-1}, follow the observed experimental size effects, i.e., the thinner the stronger, for film thicknesses h = 0.2, 0.4, and 0.6 μm. This trend reverses for the 1 μm-thick sample, which initially exhibits a response very close to the 0.6 μm-thick sample but presented a larger hardening rate after a deformation of $\approx$0.6%. The mechanism responsible for this transition is associated to the formation of dislocation networks within the grain as we will explain in subsequent paragraphs.

The DDD simulations capture the onset of plastic flow with differences in stress levels required for activation of grain boundary sources. Furthermore, the simulations for the three smaller thicknesses, i.e., for smaller aspect ratios, clearly predict a major difference in the hardening rate of the material. The responses of the 0.6- and 0.4-μm-thick films present a signifi-

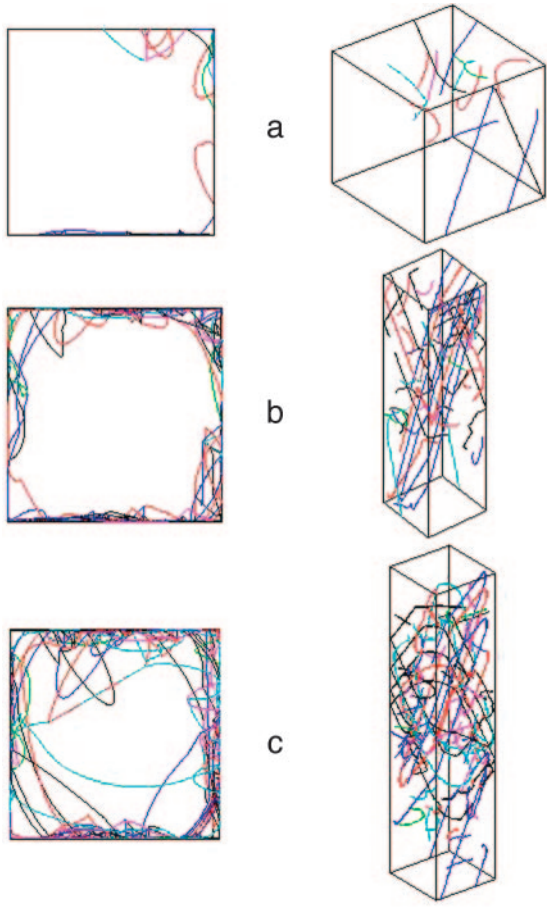

Fig. 5. Final dislocation configurations for an applied strain of 0.8% [top view (*Left*), 3D view (*Right*)]. (*a*) 0.2-μm sample. (*b*) 0.6-μm sample. (*c*) 1-μm sample.

cantly smaller hardening rate than the 0.2-μm-thick film (Fig. 4*a*). This feature reaches saturation as the grain aspect ratio is increased. To advance an explanation for this phenomenon, in Fig. 5 we plot snapshots of the dislocation structure inside the grain for the 0.2-, 0.6-, and 1-μm samples at the end of the simulation ($\varepsilon = 0.8\%$). Only the active dislocation sources are shown. Each source is active only once and then the dislocation segments are stored at the impenetrable grain boundaries or are absorbed by the free surfaces. Nucleation at each source is a one-time event because dislocation segments are not able to form a closed loop as it is the case for volume sources. This result is consistent, as highlighted in ref. 18, with deformation behavior observed in ultrafine-grained materials for which multiple dislocation pile-ups can hardly be produced.

Movies 3–5, which are published as supporting information on the PNAS web site, vividly show the evolution of dislocations. Movies 3–5 show that when the so-called grain boundary sources become active, dislocations sweep the grain and then they either intersect the surface (with some parts of the dislocation line disappearing because of the image stresses) or they are stored at the impenetrable grain boundaries. Movies 3–5 also show that dislocation interactions resulting in junctions and dislocation networks are not likely except for the high-aspect-ratio columnar grains. Our TEM observations show some evidence of formation of dislocation networks but they are present primarily in a few isolated grains exhibiting high aspect ratios (Fig. 2 *c* and *d*). These observations and the DDD simulation results are in very good agreement. Therefore, it is reasonable to conclude that the

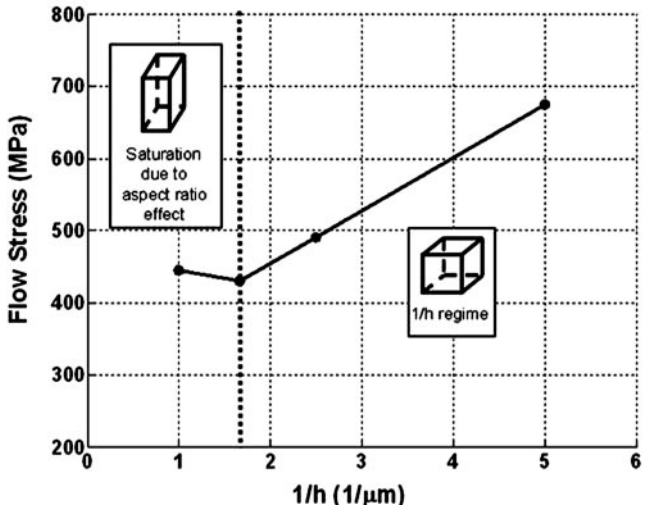

Fig. 6. Flow stress (defined as the stress corresponding to 0.2% permanent deformation upon elastic unloading) as a function of film thickness inverse.

deformation process in thin films possessing ultrafine-grained microstructures is dislocation nucleation controlled with a higher probability of source activation as the grain boundary area increases.

Our explanation of the thickness effects shown in Fig. 4*a* is then based on two facts. First, compared with the thicker films, the 0.2-μm-thick one possesses less grain boundary area and hence a lower probability of dislocation nucleation at a given stress. Second, for smaller thicknesses there is a higher probability for the dislocations to encounter free surfaces and be partially adsorbed by them, which results in a smaller available free path and consequently in a smaller potentiality for the dislocations to generate plastic strain by sweeping area inside the crystal. However, as we have already pointed out, the second effect is altered by what we have called aspect ratio effect. Indeed, for the highest aspect ratio ($h = 1$ μm, $h/d = 5$), there is a higher probability for dislocations to intersect with each other and, therefore, form junctions and networks (Fig. 5*c*). This event produces an increase of the internal stress (back stress) during the deformation process and, hence, an obstacle to further dislocation nucleation, leading to an increase in hardening rate. To validate this idea, the same simulations were performed for a smaller initial dislocation density of $\approx 0.8 \times 10^4$ cm^{-1}. The corresponding results are shown in Fig. 4*b*. As might be expected, a smaller density reduces the probability for the formation of dislocation junctions and, therefore, the saturation of the size effect is no longer manifested. This finding shows that the density of dislocation sources per unit area of grain boundary is a key parameter in determining the critical aspect ratio over which a reversal in the hardening rate is manifested. Also note that the experimental stress-strain curves obtained in freestanding f.c.c. films are more consistent with the DDD prediction based on the smallest density of source, which suggests that using such source density is more realistic.

The size-scale effects shown in Fig. 4*a* are further illustrated in Fig. 6, where the flow stress (defined as the stress corresponding to a 0.2% permanent strain) is plotted as a function of thickness inverse. For the three smallest sample sizes, we can observe a size effect in which the flow stress scales proportionally to h^{-1}. At larger thicknesses and aspect ratios, the flow stress stops decreasing and eventually starts to increase slightly as a result of the development of an internal length scale (average distance between junctions) and associated back stresses on the

potential sites for dislocation nucleation. A full discussion on back stress quantification and its implication is given in ref. 23.

In summary, two features are important in relation to the observed size-scale effects: (*i*) the onset of plastic flow, i.e., the yield stress observed on stress-strain curves and (*ii*) the plastic flow evolution, i.e., the strain-hardening rate observed in the plastic regime. In the present model, both of these features are affected by dislocation nucleation and are source-controlled. The onset of plastic flow is controlled by dislocation nucleation (weakest source activation in our model). Likewise, the plastic flow evolution in structures with small average grain sizes (100–200 nm) is also affected mainly by the probability of source nucleation at increasing stress levels especially in the early stage of deformation ($\varepsilon \leq 0.5\%$). The reason is that the "easy sources" (the ones activated at low stress states) are activated and "exhausted" in the sense that they do not contribute any further to the plastic deformation. In thin films, the availability of dislocation sources is limited as observed in *in situ* TEM experiments (10, 11). Fig. 4 shows clearly that increasing stress levels are needed to nucleate grain boundary sources of smaller size (statistical effect). Furthermore, such sources are progressively exhausted, and thus larger stress levels are required to promote further dislocation activation. In the case of millimeter-thick films (200-mm average grain size), like the ones used in our self-similar experiments (Fig. 1), even if the same number of dislocation sources per unit area are activated at a given stress and temperature, plasticity spreads in the whole grain, making a more homogeneous stress state (smaller back stresses) and allowing more source activation (see Movies 3–5). Furthermore, dislocation multiplication through activation of volume Frank-Read sources is also expected in this case (18), which is consistent with the massive plastic deformation observed experimentally (see Movies 1 and 2).

The interpretation postulated here for the observed size-scale plasticity in confined systems is based on a model that differs from prior modeling reported in the literature in several aspects. The simulations are fully three dimensional with dislocation possessing a mixed character, boundary conditions correspond to freestanding films, and the dislocation sources all are located at the grain boundaries with a realistic density and statistical distribution in size and location. It is also worth noting that some aspects linked to the mechanical behavior of polycrystalline thin films were not modeled. For instance, we did not account for the statistical distribution of grain sizes and their orientation, and we did not allow in the calculation the transmission of dislocations through grain boundaries. As such, the model proposed here is not fully quantitative of the complex plasticity size-scale phenomenon present in polycrystalline thin films. For this reason, we did not perform a one-on-one comparison with the experimental results but rather discuss trends emerging from the calculations performed with the postulated model. We believe the applicability of the model and the results inferred from it are quite general and as such are an important step forward in the interpretation of the plasticity size-scale phenomenon in small and constrained volumes. For a more quantitative analysis, the model can, in principle, be augmented and combined with atomistic and crystal plasticity models to span a larger range of size scales or make it more accurate.

We also believe that the same source-dominating processes can play a role in a variety of boundary value problems, previously solely rationalized in the context of continuum strain gradient formulations, such as in the nanoindentation experiments reported in refs. 24 and 25 and the torsion and bending experimental results given in refs. 8 and 26. In the case of nanoindentation, the roughness of the indenter and the substrate are the likely sources for dislocation nucleation (see e.g., ref. 27) and as such it could be modeled in the same spirit as the grain boundary sources modeled in this work. In the torsion and bending of wires and films, grain boundary and free surface areas scale directly with the specimen dimensions. Hence, the physics advanced in this work is likely to be of relevance to these boundary value problems as well.

We thank L. Kubin for very valuable discussions during the investigation reported here. This work was supported by National Science Foundation Grant CMS-0120866 and Army Research Office Grant W911NF-05-1-0088.

1. Masumura, R. A., Hazzledine, P. M. & Pande, C. S. (1998) *Acta Mater.* **46,** 4527–4534.
2. Van Swygenhoven, H., Caro, A. & Farkas, D. (2001) *Mater. Sci. Engin. A* **309–310,** 440–444.
3. Espinosa, H. D. & Prorok, B. C. (2001) *Mat. Res. Soc. Symp. Proc.* **695,** L8.3.1–L8.3.6.
4. Espinosa, H. D., Prorok, B. C. & Fischer, M. (2003) *J. Mech. Phys. Solids* **51,** 47–67.
5. Espinosa, H. D., Prorok, B. C. & Peng, B. (2004) *J. Mech. Phys. Solids* **52,** 667–689.
6. Uchic, M. D., Dimiduk, D. M., Florando, J. N. & Nix, W. D. (2004) *Science* **305,** 986–989.
7. Greer, J. R., Oliver, W. C. & Nix, W. D. (2005) *Acta Mater.* **53,** 1821–1830.
8. Fleck, N. A., Muller, G. M., Ashby, M. F. & Hutchinson, J. W. (1994) *Acta Metall. Mater.* **42,** 475–487.
9. Gao, H., Huang, Y., Nix, W. D. & Hutchinson, J. W. (1999) *J. Mech. Phys. Solids* **47,** 1239–1263.
10. Keller, R. R., Phelps, J. M. & Read, D. T. (1996) *Mater. Sci. Engin. A* **214,** 42–52.
11. Haque, M. A. & Saif, M. T. A. (2002) *Sensors Actuators A* **97–98,** 239–245.
12. Hutchinson, J. W. (2000) *Int. J. Solids Struct.* **37,** 225–238.
13. Nicola, L., Van der Giessen, E. & Needleman, A. (2003) *J. Appl. Phys.* **93,** 5920–5928.
14. Von Blanckenhagen, B., Arzt, E. & Gumbsch P. (2004) *Acta Mater.* **52,** 773–784.
15. Madec, R., Devincre, B., Kubin, L., Hoc, T. & Rodney, D. (2003) *Science* **301,** 1879–1882.
16. Schwarz, K. W. (1999) *J. Appl. Phys.* **85,** 108–119.
17. Schwarz, K. W. (2003) *Model. Simul. Mater. Sci. Engin.* **11,** 609–625.
18. Cheng, S., Spencer, J. A. & Milligan, W. W. (2003) *Acta Mater.* **51,** 4505–4518.
19. Legros, M., Dehm, G., Balk, T. J., Arzt, E., Bostrom, O., Gergaud, P., Thomas, O. & Kaouache, B. (2003) *Mater. Res. Soc. Symp. Proc.* **779,** W4.2.1–W4.2.12.
20. Balk, T. J., Dehm, G. & Arzt, E. (2001) *Mater. Res. Soc. Symp. Proc.* **673,** P2.7.1–P2.7.6.
21. Schiotz, J. (2004) *Scripta Mater.* **51,** 837–841.
22. Farkas, D. & Curtin, W. A. (2005) *Mater. Sci. Engin.*, in press.
23. Espinosa, H. D., Panico, M., Berbenni, S. & Schwarz, K. W. (2005) *Int. J. Plasticity*, in press.
24. Ma, Q. & Clarke, D. R. (1995) *J. Mater. Res.* **10,** 853–863.
25. Nix, W. D. & Gao, H. (1998) *J. Mech. Phys. Solids* **46,** 411–425.
26. Stölken, J. S. & Evans, A. G. (1998) *Acta Mater.* **46,** 5109–5115.
27. Yu, H. H., Shrotriya, P., Wang, J. & Kim, K. S. (2003) *Mater. Res. Soc. Symp. Proc.* **795,** U7.9.1–U7.9.6.